

# Amplified spontaneous emission at 5.23 $\mu\text{m}$ in two-photon excited Rb vapour

A.M. Akulshin<sup>1</sup>, N. Rahaman<sup>1</sup>, S.A. Suslov<sup>2</sup> and R.J. McLean<sup>1</sup>

<sup>1</sup>Centre for Quantum and Optical Science, Swinburne University of Technology,  
PO Box 218, Melbourne 3122, Australia

<sup>2</sup>Department of Mathematics, Faculty of Science, Engineering and Technology,  
Swinburne University of Technology, Melbourne 3122, Australia

Version 1 January 2017

## Abstract

Population inversion on the  $5D_{5/2} \rightarrow 6P_{3/2}$  transition in Rb atoms produced by cw excitation at different wavelengths has been analysed by comparing the generated mid-IR radiation at 5.23  $\mu\text{m}$  originated from amplified spontaneous emission and isotropic blue fluorescence at 420 nm. A novel method of detecting two-photon excitation in atomic vapours using ASE is suggested. We have observed directional co- and counter-propagating emission at 5.23  $\mu\text{m}$ . We find that the power dependences of the backward- and forward-directed emission can be very close, however their spectral dependences are not identical. The mid-IR emission in Rb vapours excited by nearly counter-propagating beams at 780 and 776 nm does not exactly coincide spatially with the applied laser beams. The presented observations could be useful for enhancing efficiency of frequency mixing processes and new field generation in atomic media.

## 1. Introduction

The interest in frequency conversion of cw resonant light and laserlike new field generation in atomic media specially prepared by resonant laser light is driven by a number of possible applications [1, 2, 3, 4]. The transfer of population to excited levels, particularly to create population inversion on strong transitions in the optical domain, is an essential part of the nonlinear process of frequency up- and down-conversion [5, 6, 7].

For example, two-photon excitation of Rb atoms from the ground state to the  $5D_{5/2}$  level using laser fields at different wavelengths, as shown in Figure 1, produces population inversion on the three cascade one-photon transitions  $5D_{5/2} \rightarrow 6P_{3/2}$ ,  $6P_{3/2} \rightarrow 6S_{1/2}$  and  $6S_{1/2} \rightarrow 5P_{1/2}$  since in each case the upper energy level has a longer lifetime than the lower level. If both the two-photon excitation rate and the atom number density  $N$  are sufficiently high to produce more than one stimulated photon per spontaneous photon, then amplified spontaneous emission (ASE) might occur [8, 9]. In the highly-elongated interaction region defined by the applied laser beams this leads to directional stimulated emission at 1.32  $\mu\text{m}$  and 5.23  $\mu\text{m}$  [10, 11]. Intensities of these internally generated fields can be high enough to establish coherence between different states and subsequent parametric mixing with the applied laser radiation that produces coherent emission at 420 nm and 1.37  $\mu\text{m}$  [5-7, 11] in directions allowed by the phase-matching condition [6].

Obviously, such process resulting in directional ASE could occur in other atomic species under appropriate laser excitation. Probably the first laser-induced two-photon stimulated emission in pulsed and cw two-photon excited mercury vapours were observed in [12, 13], respectively.

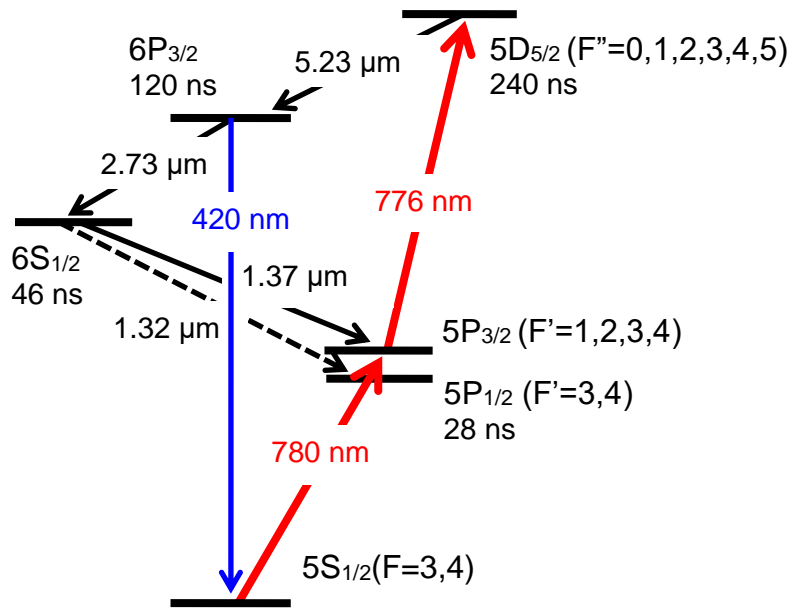


**Figure 1.**  $^{85}\text{Rb}$  atom energy levels involved in cascade population inversion.

In this paper, we report on an experimental investigation of the mid-IR radiation at  $5.23\ \mu\text{m}$  generated due to the ASE process in two-photon excited Rb vapour. Spatial and spectral properties of ASE are defined to a large extent by the geometry of the region that contains population-inverted atoms [14]. While the intensity of isotropic resonant fluorescence is a good local indicator of the number of excited Rb atoms, the directional radiation originating from ASE provides complementary information about excited atoms integrated over the light-atom interaction region. ASE could also provide a signal with a higher signal-to-noise ratio compared to isotropic fluorescence when population inversion is prepared in a pencil-shaped interaction region within dilute vapours.

We note that similar energy level configurations in Rb atoms have been used extensively for studying ladder-type EIT [15], atomic coherence effects [16], as well as for imaging of ultracold atoms [17].

## 2. Two-photon excitation: General consideration

Doppler-free two-photon excitation [18] in alkali atoms is usually detected by observing isotropic fluorescence emitted during cascade decay. Typically, the collected fluorescence and applied laser light are spectrally separated, dramatically simplifying the detection procedure. Other popular methods are based on detecting absorption or polarization rotation of the applied laser light transmitted through an atomic sample [19, 20, 21]. Detection of new optical fields generated by ASE is less common [22].

There are two distinct ways of exciting Rb atoms to the  $5D_{5/2}$  level using low-intensity cw resonant laser light at 780 and 776 nm.

- Two-photon nearly velocity-insensitive excitation

The excitation from the ground state to the  $5D_{5/2}$  level can occur by absorbing two photons instantaneously when their sum frequency is resonant with the two-photon transitions  $\nu_{780} + \nu_{776} = \nu_{FF''}$ , where  $\nu_{FF''}$  are the frequencies of the two-photon transitions between the  $5S_{1/2}$  and  $5D_{5/2}$  hyperfine levels  $F$  and  $F''$ , respectively.

In the case of counter-propagating beams at 780 and 776 nm, nearly the whole velocity distribution of Rb atoms interacts simultaneously with the applied laser light at the two-photon resonance, as the Doppler shift for moving atoms is almost compensated for the laser beams of similar wavelength:

$$(\nu_{780} + \nu_{776}) - (k_{780} - k_{776})V/2\pi \approx \nu_{FF'}, \text{ as } k_{780} \approx k_{776},$$

where  $k_{780}$  and  $k_{776}$  are the wave numbers at the appropriate wavelengths.

The two-photon excitation is strongly enhanced when both optical frequencies are individually resonant to the one-photon transitions [23, 24].

- Velocity-selective excitation

Instead of the velocity insensitive excitation, Rb atoms can be also excited to the  $5D_{5/2}$  level within a certain velocity group. Indeed, if the co-propagating laser beams at 780 and 776 nm have approximately equal frequency detuning  $\delta < \Delta\nu_D$  from the corresponding one-photon transitions, where  $\Delta\nu_D$  is the Doppler width, atoms having  $V = 2\pi\delta/k$  velocity projection on the laser beam direction are at the two-photon resonance with the applied laser light despite the detuned sum frequency:

$$(\nu_{780} + \nu_{776}) - \nu_{FF'} = (k_{780} + k_{776})V/2\pi.$$

In this velocity group Rb atoms could be excited to the  $5D_{5/2}$  level by both incoherent stepwise and coherent two-photon processes [23]. Numerical modelling of the corresponding excitation in Cs atoms shows that the contribution of the two-photon process prevails at high power [20].

In Rb vapours, narrow-linewidth fixed-frequency laser light at 780 nm that is tuned to the inhomogeneously broadened  $^{85}\text{Rb}$ -D2 absorption line interacts with atoms having certain velocity projections on the laser beam direction. Their velocity projections  $V_{FF'}$  are determined by the frequency detuning of the laser  $\nu_{780}$  from the corresponding resonant frequencies  $\nu_{FF'}$  of the  $5S_{1/2}(F=2; 3) \rightarrow 5P_{3/2}(F'=2; 3; 4)$  hyperfine manifold:

$$V_{FF'} = 2\pi(\nu_{780} - \nu_{FF'})/k_{780}.$$

Under our experimental conditions when the 780 nm laser is tuned to the  $5S_{1/2}(F=3) \rightarrow 5P_{3/2}$  manifold, the number of atoms in the  $5S_{1/2}(F=3)$  level in the  $V_{32}$  and  $V_{33}$  velocity groups is significantly reduced compared to the initial steady-state level due to optical re-pumping to the  $5S_{1/2}(F=2)$  level. Thus, Rb atom excitation to the intermediate  $5P_{3/2}$  level predominantly occurs via the strongest cycling  $5S_{1/2}(F=3) \rightarrow 5P_{3/2}(F'=4)$  transition, as was shown in [25] and the insignificant numbers of excited atoms in the  $V_{32}$  and  $V_{33}$  velocity groups are ignored in the following consideration.

### 3. Experimental setup

The experimental arrangement is similar to that used previously for studying the two-photon spectroscopy [26] and directional polychromatic light generation [11] in Rb vapours.

Rb atoms are excited from the ground state to the  $5D_{5/2}$  level by the optical fields from two extended-cavity diode lasers at 780 and 776 nm. The lasers are tuned close to the strong  $5S_{1/2}(F=3) \rightarrow 5P_{3/2}$  and  $5P_{3/2} \rightarrow 5D_{5/2}$  transitions in  $^{85}\text{Rb}$  (Figure 1). An additional laser tuned to the Rb-D1 line provides resonant radiation for ground-state re-pumping.

A gas of the natural mixture of Rb isotopes is contained in a 5-cm long heated glass cell with 1-mm thick sapphire windows, which are partially transparent at 5.23  $\mu\text{m}$ . The temperature of the cell is set within the range 45-85°C, so that the atomic density  $N$  of saturated Rb vapour could be varied approximately between  $1 \times 10^{11} \text{ cm}^{-3}$  and  $12 \times 10^{11} \text{ cm}^{-3}$  [27].

Rb atoms contained in the cell are simultaneously excited by the two-color beam that contains carefully superimposed radiation at 780 and 776 nm and the counter-propagating laser beam at 776 nm (Figure 2a). The laser power of all beams is controlled with wave plates and polarization beam splitters (PBS). The diameters of the nearly parallel beams are approximately 1.4 mm. The maximum laser power of all beams before entering the cell with sapphire windows does not exceed 3 mW, so that the Rabi frequency  $\Omega$  of the applied laser fields are  $\gamma < \Omega < \Delta\nu_D$ , where  $\gamma$  is natural linewidth of one-photon transitions.

A room-temperature photovoltaic detector based on a variable-gap HgCdTe semiconductor with 1x1 mm light-sensitive area allows the 5.23  $\mu\text{m}$  radiation to be detected using a lock-in amplifier.

The isotropic blue fluorescence at 420 nm is detected at right angles with respect to the direction of the applied laser beams by a photomultiplier tube (PMT). The blue fluorescence is separated from the laser radiation and near-infrared fluorescence by colour filters.

The cell orientation is such that the reflection of applied laser light from the cell windows does not overlap with the incident beams. We find that birefringence of the sapphire cell windows results in minor polarization distortions of the transmitted laser light.

In our experiment, the ASE and blue fluorescence are recorded as a function of the optical frequency of either of the lasers while the frequency of the other laser remains fixed. Spatial profiles of the mid-IR emission are recorded using frequency-stabilized laser fields.

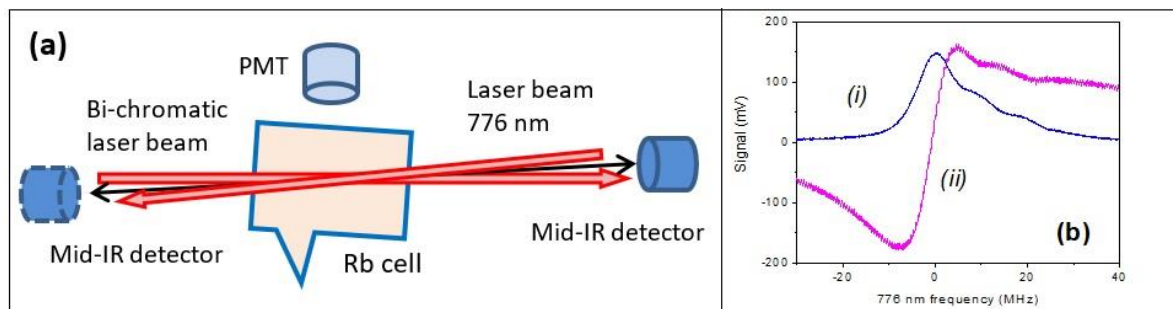


**Figure 2.** a) Simplified optical scheme of the experiment. b) Spectral dependence of (i) isotropic blue fluorescence and (ii) polarization signal for frequency locking of the 776 nm laser observed in an additional Rb cell in the vicinity of the two-photon  $5S_{1/2}(F=3) \rightarrow 5D_{5/2}(F'')$  transitions, while the frequency of the 780 nm laser is modulation-free locked to the  $5S_{1/2}(F=3) \rightarrow 5P_{3/2}(F'=4)$  transition.

Polarization spectroscopy provides a convenient signal for modulation-free laser frequency locking not only to the strong D-lines, but also to optical transitions between excited energy levels. As was shown in [26], the polarization resonances, which occur when the sum frequency of the 780 and 776 nm laser fields ( $\nu_{780} + \nu_{776}$ ) is equal to the frequencies of the two-photon  $5S_{1/2}(F) \rightarrow 5D_{5/2}(F'')$  transitions ( $\nu_{780} + \nu_{776} = \nu_{FF''}$ ), can be used as a reference for sum-frequency stabilization using a single servo system. Birefringence in the Rb vapour in the vicinity of the two-photon transition is induced by the circularly polarized beam at 780 nm. The linear polarization of the counter-propagating probe beam at 776 nm is tilted by approximately 45 degrees with respect the PBS. The

transmitted probe beam is decomposed into vertically and horizontally polarized components by the PBS, which are detected by two photodiodes, as was done in [28]. Their outputs are fed to a differential amplifier to produce a dispersion-shaped signal with an adjustable dc level for the servosystem (Figure 2b).

Sum frequency stabilization alone is not sufficient to ensure the intensity-stable mid-IR directional emission as the excitation efficiency depends on frequency detuning from the one-photon transitions. Thus, the optical frequency of the 780 nm laser is also stabilized using polarization Doppler-free resonance on the closed  $5S_{1/2}(F=3) \rightarrow 5P_{3/2}(F'=4)$  transition or to the nearest cross over resonance ensuring that  $\nu_{780} = \nu_{34}$  or red detuned  $\nu_{780} \approx \nu_{34} - 60$  MHz, respectively.

Laser frequency stabilization results in reduced low-frequency variation of the number of two-photon excited Rb atoms, more stable blue fluorescence as well as ASE. The measured relative intensity instability of the isotropic fluorescence at 420 nm within a 60 s time interval is less than 0.5%.

#### 4. Experimental observations

Figure 3a shows typical spectral dependences of the forward-directed mid-IR radiation at  $5.23 \mu\text{m}$  and isotropic blue fluorescence at 420 nm if the fixed frequency 780 nm laser is detuned from the  $5S_{1/2}(F=3) \rightarrow 5P_{3/2}(F'=4)$  transition,  $\nu_{780} - \nu_{34} < \Delta\nu_D$ . Both the dependences, recorded simultaneously, reveal two-peak structures. The broader, weaker peaks are the result of velocity-selective excitation produced by the co-propagating fields at 780 and 776 nm, while the stronger and narrower peaks are due to two-photon excitation produced by the combination of the 780 nm component of the two-colour beam and the counter-propagating radiation at 776 nm. Also, both the mid-IR resonances originating from ASE on the population inverted transition are noticeably narrower than the fluorescence peaks. We attribute this observation to a gain effect in the population-inverted medium.

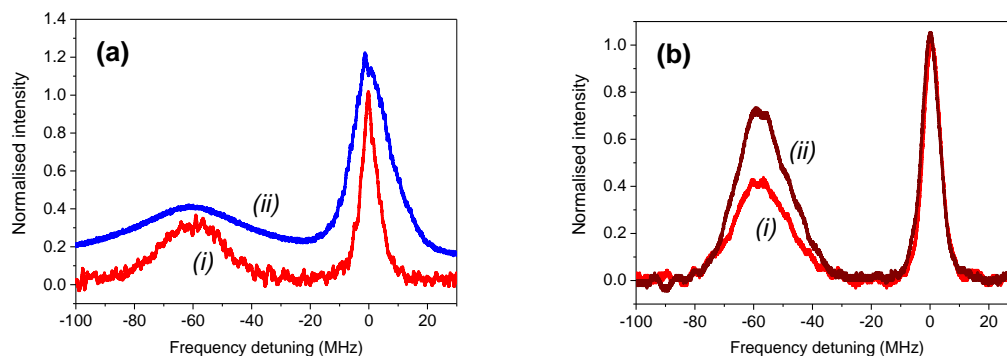


**Figure 3. (a)** Forward-directed ASE at  $5.23 \mu\text{m}$  (i) and (ii) isotropic blue fluorescence at 420 nm (offset vertically by 0.2 divisions for clarity) as functions of the frequency detuning of the 776 nm laser from the two-photon resonance ( $\nu_{780} + \nu_{776} = \nu_{35}$ ), while the fixed frequency 780 nm laser is approximately 60 MHz red-detuned from the  $5S_{1/2}(F=3) \rightarrow 5P_{3/2}(F'=4)$  transition.

**(b)** Forward-directed ASE at  $5.23 \mu\text{m}$  (i) without and (ii) with an additional re-pumping co-propagating beam ( $I \approx 2 \text{ mW/cm}^2$ ) that is tuned to the  $5S_{1/2}(F=2) \rightarrow 5P_{1/2}(F'=3)$  transition as a function of the 776 nm laser detuning from the two-photon resonance on the  $5S_{1/2}(F=3) \rightarrow 5D_{5/2}(F''=5)$  transition. The 780 nm laser is locked approximately 60 MHz red-detuned from the  $5S_{1/2}(F=3) \rightarrow 5P_{3/2}(F'=4)$  transition.

To emphasise the difference between the velocity-selective and velocity-insensitive excitations, we apply a re-pumping laser beam in the co-propagating direction. A similar method was used for

controlling nonlinear mixing processes and coherent blue light generation in alkali vapours [25]. If this laser light tuned to the Rb-D1 line is sufficiently intense ( $I > h\nu/\sigma_0 T$ , where  $\sigma_0$  is the absorption cross section of the transition in the  $5S_{1/2} \rightarrow 5P_{1/2}$  manifold and  $T$  is the interaction time determined by the beam diameter and the most probable velocity of Rb atoms [29]), the fixed frequency laser field  $\nu_{D1}$  tuned to the vicinity of the open  $5S_{1/2}(F=2) \rightarrow 5P_{1/2}(F'=2, 3)$  transitions produces efficient population pumping from the lower  $F=2$  to the upper  $F=3$  ground-state level in two velocity groups:

$$V_{OP}' = 2\pi(\nu_{D1} - \nu_{23})/k_{D1} \text{ and } V_{OP}'' = 2\pi(\nu_{D1} - \nu_{22})/k_{D1},$$

where  $V_{OP}$  is velocity projection onto the direction of the laser beam and  $k_{D1}$  is the wave number of the 795 nm laser radiation.

As the initial steady-state population of the ground-state levels before interacting with light are proportional to their degeneracy  $g_F = 2F+1$ , such pumping could produce up to  $g_2/g_3 = 5/7 \approx 70\%$  enhancement of the number of atoms in the resonant velocity group on the  $F=3$  level, assuming complete transfer from  $F=2$  to  $F=3$  ground hyperfine levels.

Thus, the number of atoms excited to the  $5D_{5/2}$  level is increased if the 795 nm laser is tuned to interact with the same velocity group as the 780 nm laser ( $V_{OP} = 2\pi(\nu_{780} - \nu_{34})/k_{780} = 2\pi(\nu_{D1} - \nu_{23})/k_{D1}$ ). This in its turn enhances both the velocity-selective and velocity-insensitive ASE peaks, as Figure 3b demonstrates. However, the enhancements due to velocity selective optical pumping are different for the two methods of excitation. The velocity-selective peak is increased by approximately 70%, i.e. very close to the maximum possible population increase in the resonant velocity group on the  $F=3$  level. The velocity-insensitive or unmixed two-photon ASE peak that is proportional to the total number of atoms regardless of their velocity projection is enhanced by approximately 3%, as the number of pumped atoms compared to the total population of the  $F=3$  level is small, approximately  $\Gamma/\Delta\nu_D$ , where  $\Gamma$  is the homogeneous linewidth and in our experiment  $\Gamma/\Delta\nu_D \approx 20$ .

If the 780 nm and 795 nm laser fields interact with different velocity groups within the Doppler profile,  $(\nu_{780} - \nu_{34})/k_{D2} \neq (\nu_{D1} - \nu_{23})/k_{D1}$ , the velocity selective peak is unchanged from the no D1-line re-pumping case, because the population of the  $V = 2\pi(\nu_{780} - \nu_{34})/k_{D2}$  velocity group in the  $F=3$  level is not increased, while the enhancement of the two-photon ASE peak depends weakly of the 795 nm laser detuning, as the total population in the  $F=3$  level is increased. Thus, the tuning of the optical re-pumping laser is not critical for the exact two-photon ASE, but the mixed ASE peak originated from both stepwise and two-photon excitation processes is very sensitive to the re-pumping frequency.

Although in general the enhancement is not proportional to the increase in the number of resonant Rb atoms because of the threshold-like behaviour of the ASE, the ground-state hyperfine optical pumping observation does clearly demonstrate the difference between the velocity selective and velocity insensitive excitation to the  $5D_{5/2}$  level using laser light at 780 and 776 nm.

It is worth noting that the velocity-selective two-wavelength excitation in Cs vapours ( $6S_{1/2} \rightarrow 6P_{3/2} \rightarrow 6D_{5/2}$ ) was quantitatively analysed in [30]. It was shown that only approximately 1% of the ground state population could reach the  $6D_{5/2}$  using cw narrow-linewidth lasers.

In the spectral dependences presented in Figure 3a, the closely-spaced hyperfine structure of the  $^{85}\text{Rb}$   $5D_{5/2}$  level is not resolved mainly due to power broadening. At lower laser power the two-photon peak of blue fluorescence reveals a partly resolved structure that corresponds to the excitation of  $^{85}\text{Rb}$  atoms from the  $5S_{1/2}(F=3)$  to  $5D_{5/2}(F'')$  levels allowed by the two-photon selection rule  $\Delta F = |F - F''| \leq 2$  for the case of two photons with different frequencies [31], as shown in Figures 4.

However, the forward-directed ASE occurs only in the vicinity of the strongest two-photon ( $F = 3$ )  $\rightarrow$  ( $F'' = 5$ ) transition (Figure 4a).

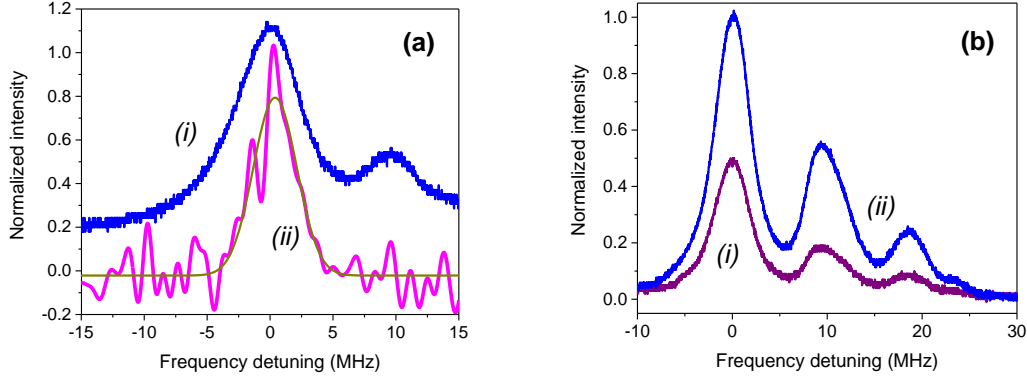


**Figure 4.** (a) Spectral dependence of (i) the blue fluorescence of the two-photon excited  $^{85}\text{Rb}$  atoms and the forward-directed ASE at  $5.23\ \mu\text{m}$  at low laser intensity ( $I < 1\ \text{mW}/\text{cm}^2$ ). The  $780\ \text{nm}$  laser is locked approximately  $60\ \text{MHz}$  red-detuned from the  $5S_{1/2}(F=3) \rightarrow 5P_{3/2}(F'=4)$  transition.

(b) Spectral dependence of (i) backward-directed and (ii) transverse blue fluorescence on the  $5S_{1/2}(F=3) \rightarrow 5D_{5/2}(F'')$  manifold.

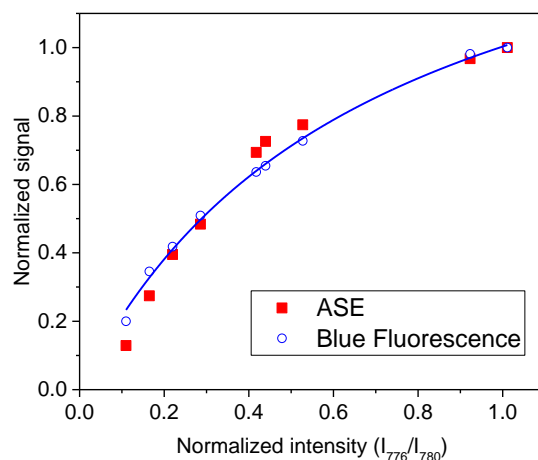
The minimal observed full width at half maximum (FWHM) of the two-photon ASE resonance at such low intensity of the applied laser fields is approximately  $4\ \text{MHz}$ . The ultimate linewidth of the two-photon resonances produced by the monochromatic excitation is defined by a sum of the initial and final state decay rate  $\gamma_S + \gamma_D$ , where  $\gamma_D \approx 2\pi \times 0.66\ \text{MHz}$  and  $\gamma_S$  is determined by the time of flight of atoms across the laser beams. In the present case, these resonances are additionally broadened due to a mismatch in Doppler shifts  $(\nu_{776}/\nu_{780} - 1)\Delta\nu_D \approx 2.5\ \text{MHz}$  arising from the frequency difference of the two optical fields.

We note that spectral dependences of blue fluorescence detected in transverse and in the counter-propagating directions are practically identical (Figure 4b), while in the co-propagating direction the emission at  $420\ \text{nm}$  might occur in a form of intense spatially and temporally coherent light generated by parametric FWM [6-7]. The similar spectral profiles of backward-directed and transverse blue fluorescence clearly indicate that the emission at  $420\ \text{nm}$  remains entirely spontaneous as the phase matching condition is not satisfied. Also the backward blue emission, unlike the mid-IR radiation, is not amplified after propagation through the medium because the  $5S_{1/2}(F=3) \rightarrow 6P_{3/2}$  transition is not population inverted.

Figure 5 shows the intensity of the forward-directed emission at  $5.23\ \mu\text{m}$  and isotropic blue fluorescence as functions of the laser power at  $776\ \text{nm}$ . The dependences are similar and demonstrate a pronounced saturation characteristic. The saturation parameters  $I_{SAT}$  evaluated via fitting the experimental data to the  $I/(1+I/I_{SAT})$  dependence are close,  $63 \pm 4$  and  $67 \pm 13\ \text{mW}/\text{cm}^2$  for the isotropic blue fluorescence and mid-IR emission, respectively. A detailed study of the dynamic Stark effect and power broadening of the ASE resonances is the subject of a following paper.

The presented power dependence of the ASE does not reveal a steep power increase that typically occurs when the directional radiation appears from the isotropic spontaneous emission [9, 9]. This clearly indicates that the observations have been done above the ASE threshold. The sensitivity of our detection system is not high enough to observe the isotropic fluorescence at  $5.23\ \mu\text{m}$  and the onset of the directional mid-IR radiation, i.e. the ASE threshold. The low collection efficiency results from the lack of a suitable lens for focusing for the  $5.23\ \mu\text{m}$  radiation and the small solid angle of the mid-IR detector.

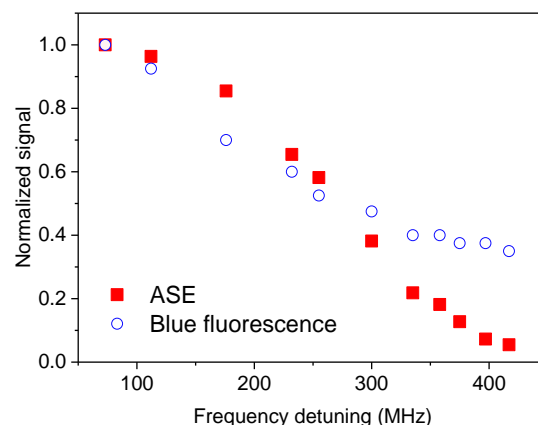
It is also worth noting that two-photon excitation and subsequent ASE at 5.23  $\mu\text{m}$  could occur even with a large intensity imbalance between the counter-propagating beams at 780 and 776 nm.



**Figure 5.** Normalized ASE at 5.23  $\mu\text{m}$  and isotropic blue fluorescence and recorded simultaneously as a function of the 776 nm beam normalized power. The mid-IR emission is detected in the direction of the 780 nm beam. Optical frequency of the 780 nm laser is locked approximately 60 MHz red-detuned from the  $5S_{1/2}(F=3) \rightarrow 5P_{3/2}(F'=4)$  transition, while the 776 nm laser is locked to the two-photon resonance on the  $5S_{1/2}(F=3) \rightarrow 5D_{5/2}(F''=5)$  transition.

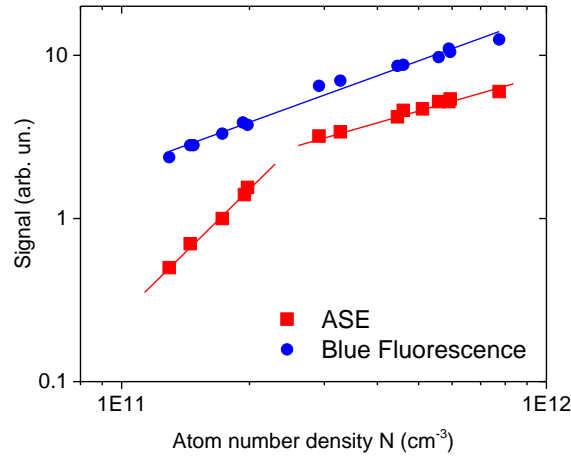
In Figure 6 we compare the variations of the isotropic blue fluorescence and the mid-IR emission detected in the direction of the 780 nm beam as a function of frequency detuning of the 780 nm laser above the strongest  $5S_{1/2}(F=3) \rightarrow 5P_{3/2}(F'=4)$  transition. High-frequency detuning is chosen to make contributions to the two-photon excitation from the weaker  $5S_{1/2}(F=3) \rightarrow 5P_{3/2}(F'=2; 3)$  transitions negligible. The dependences are taken simultaneously at the atom number density  $N \approx 5 \times 10^{11} \text{ cm}^{-3}$ .

Figure 6 shows that the mid-IR emission decays much faster with  $\delta$ ; at  $\delta > 400$  MHz the ASE signal is below the detection limit, while the blue fluorescence is still rather strong.



**Figure 6.** ASE emission originated from velocity-insensitive two-photon excitation and isotropic blue fluorescence detected simultaneously as a function of high frequency detuning of the 780 nm laser from the  $5S_{1/2}(F=3) \rightarrow 5P_{3/2}(F'=4)$  transition,  $\delta = \nu_{780} - \nu_{34}$ , providing that the sum of laser frequencies ( $\nu_{780} + \nu_{776}$ ) matches the frequency of the  $5S_{1/2}(F=3) \rightarrow 5D_{5/2}(F''=5)$  two-photon transition. ASE at 5.23  $\mu\text{m}$  is detected in the direction of the 780 nm beam.





**Figure 7.** Two-photon ASE and isotropic blue fluorescence as a function of Rb number density  $N$ . Mid-IR light is detected in the direction of the 780 nm beam. The 780 nm laser is approximately 60 MHz red-detuned from the  $5S_{1/2}(F=3) \rightarrow 5P_{3/2}(F'=4)$  transition, while the 776 nm laser is locked to the two-photon resonance on the  $5S_{1/2}(F=3) \rightarrow 5D_{5/2}(F''=5)$  transition.

Figure 7 demonstrates the Rb number density dependence of the two-photon ASE and isotropic blue fluorescence. Linear fits to the experimental data presented in the log-log plot reveal that the isotropic blue fluorescence is proportional to the Rb number atomic density  $N$  ( $\sim N^\beta$ , where  $\beta = 0.95 \pm 0.04$ ), while the ASE demonstrates much steeper rise ( $\beta = 2.3 \pm 0.2$ ) at lower Rb number density ( $N < 1.1 \times 10^{11} \text{ cm}^{-3}$ ) followed by the region of the linear growth.

The observation of blue fluorescence without detecting mid-IR emission at  $5.23 \mu\text{m}$  at some experimental conditions, such as large frequency detuning  $\delta$  or low atom number density  $N$ , might seem counterintuitive, as the population transfer from the  $5D_{5/2}$  to  $6P_{3/2}$  levels implies mid-IR photons are emitted. This could be explained simply by different mid-IR and blue fluorescence detection thresholds. The intensity of directional radiation at  $5.23 \mu\text{m}$  is below our detection limit, but it is present, and results in blue fluorescence that is detected with much higher efficiency. Indeed, the detected blue fluorescence might result entirely from spontaneous process on the  $5D_{5/2} \rightarrow 6P_{3/2}$  transition, while the detection sensitivity is not sufficient to detect the isotropic fluorescence at  $5.23 \mu\text{m}$ .

Analysing directionality of the mid-IR emission, we find that in Rb vapours two-photon excited by counter-propagating fields at 780 and 776 nm crossing at a small angle, the direction of maximum emission does not coincide with the laser beams. The maximum ASE occurs in the direction of max extent of the gain region, as shown in Figure 8.

We find that under a range of experimental conditions the backward- and forward-directed ASE generated in two-photon excited Rb vapours are equally intense and exhibit similar power dependences. The plots of spectral dependences of ASE in the backward and forward directions are shown in Figure 9. Despite very similar intensities observed in both directions, their spectral profiles are not identical. The mid-IR emission in the direction of the 776 nm beam is shifted toward lower frequencies by approximately half the width of the spectral profile.

A similar imbalance was observed in three-photon pumped argon-air mixtures [32] and attributed to the asymmetry of the gain in the gain region. It has also been suggested that the backward- and forward-propagating emissions compete for gain [33].

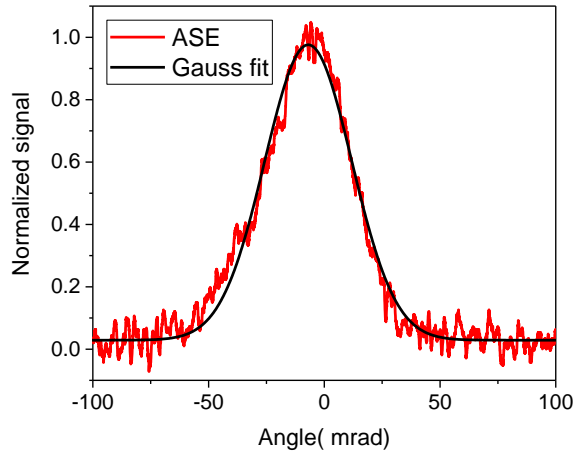


**Figure 8.** Spatial profile of ASE produced by nearly counter-propagating laser beams at 780 nm and 776 nm fitted to a Gaussian curve. The crossing angle  $\theta$  is approximately 7.5 mrad.

The distinctive spectral and intensity features of the laser-like backward and forward emission in Rb vapour excited simultaneously by stepwise and two-photon process or entirely via the resonant two-photon process merit more detailed investigation because of their possible applicability to remote sensing. We note that the velocity-selective population inversion on the  $5D_{5/2} \rightarrow 5P_{3/2}(F=3)$  transition that is produced by the co-propagating laser beams at 780 and 776 nm results in very distinctive power dependences in the co- and counter-propagating directions [11].

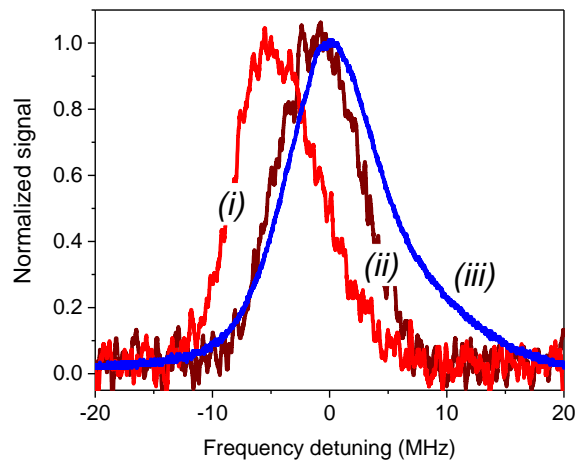


**Figure 9.** Spectral dependence of two-photon ASE generated in Rb vapours excited by counter-propagating laser beams. Curves (i) and (ii) represent the radiation at  $5.23 \mu\text{m}$  detected in the direction of the 776 nm and 780 nm beams, respectively, while curve (iii) shows the variation of isotropic blue fluorescence.

Thus, distinctive spectral and intensity features of the laserlike backward and forward emission in Rb vapour excited simultaneously stepwise and by the two-photon process or entirely via the resonant two-photon process deserve a more detail investigation because of possible practical outcomes for remote sensing.

## 5. Conclusions

Population inversion on the  $5D_{5/2} \rightarrow 6P_{3/2}$  transition in Rb atoms produced by two-photon excitation at different wavelengths has been analysed by comparing mid-IR emission at  $5.23 \mu\text{m}$  and isotropic blue fluorescence at  $420 \text{ nm}$ . The intensity of isotropic resonant fluorescence is a good local indicator of the number of excited Rb atoms, the directional radiation originating from ASE provides complementary information about excited atoms integrated over the light-atom interaction region.

It is shown that depending on the geometry of the applied radiation at  $780$  and  $776 \text{ nm}$  the excitation could be velocity-selective or velocity-insensitive, producing spectrally and spatially distinguishable directional radiation at  $5.23 \mu\text{m}$  via the mechanism of ASE. Thus, a new way of detecting two-photon excitation in atomic vapours using ASE is suggested.

Specific features of velocity-insensitive and velocity-selective excitation have been emphasised using a ground-state population re-pumping approach.

Intensity dependences of directional mid-IR emission at  $5.23 \mu\text{m}$  and isotropic blue fluorescence at  $420 \text{ nm}$  reveal a saturation characteristic. We find that the saturation intensities for both cases are similar.

The directional emission at  $5.23 \mu\text{m}$  in Rb vapours excited by nearly counter-propagating beams at  $780$  and  $776 \text{ nm}$  occurs in both directions but not exactly coinciding with the applied laser beams.

Spectral profiles of ASE for both the velocity-selective and velocity-insensitive excitation are narrower than the corresponding resonances of isotropic blue fluorescence, which is that is attributed to the amplification effect. The smallest observed full width of the two-photon ASE resonance is approximately  $4 \text{ MHz}$ .

Analysing intensity and spectral dependences confirms that the directional mid-IR radiation is due to stimulated process on a population-inverted transition, while the isotropic blue fluorescence originates from spontaneous relaxation.

Better understanding the specific properties of directional mid-IR emission could result in enhanced efficiency of frequency mixing processes and new field generation in atomic media.

Finally, ASE-based detection might be more suitable for single-sided remote sensing, as this emission occurs in both forward and backward directions. The mechanism of ASE described here could be easily extended to other atomic species allowing generation of coherent fields at exotic wavelengths.

## Acknowledgments

The authors are grateful to Dmitry Budker for his interest, as well as for the loan of the Rb cell with sapphire windows and the mid-IR detector. AA also warmly thanks Tatiana Tchernova for technical assistance.

---

<sup>1</sup> T. Hebert, R. Wannemacher, W. Lenth, and R. M. Macfarlane, *Appl. Phys. Lett.* **57**, 1727 (1990).

<sup>2</sup> A. G. Radnaev, Y. O. Dudin, R. Zhao, H. H. Jen, S. D. Jenkins, A. Kuzmich, T. A. B. Kennedy, *Nature Phys.* **6**, 894 (2010).

<sup>3</sup> G. Walker, A. S. Arnold, and S. Franke-Arnold, *Phys. Rev. Lett.* **108**, 243601 (2012).

<sup>4</sup> W. Krupke, R. Beach, V. Kanz, and S. Payne, *Opt. Lett.* **28**, 2336 (2003).

<sup>5</sup> A. S. Zibrov, M. D. Lukin, L. Hollberg, and M. O. Scully, *Phys. Rev. A* **65**(5), 051801 (2002).

<sup>6</sup> A. M. Akulshin, R. J. McLean, A. I. Sidorov, and P. Hannaford, *Opt. Express* **17**, 22861 (2009).

- 
- <sup>7</sup> A. Vernier, S. Franke-Arnold, E. Riis, A. S. and Arnold, *Opt. Express* **18**, 17026 (2010).
- <sup>8</sup> G. I. Peters and L. Allen, *J. Phys. A: Gen. Phys.* **4**, 238 (1971).
- <sup>9</sup> L. W. Casperson, *J. Appl. Phys.* **48**, 256 (1977).
- <sup>10</sup> J. F. Sell, M. A. Gearba, B. D. DePaola, and R. J. Knize, *Opt. Lett.* **39**, 528 (2014).
- <sup>11</sup> A. Akulshin, D. Budker, and R. McLean, *Opt. Lett.* **39**, 845 (2014).
- <sup>12</sup> N. Omenetto, O. I. Matveev, W. Resto, R. Badini, B. W. Smith, and J. D. Winefordner, *Appl. Phys. B* **58**, 303 (1994).
- <sup>13</sup> D. Kolbe, M. Scheid, A. Koglbauer, and J. Walz *Opt. Lett.* **35**, No. 16, 2690 (2010).
- <sup>14</sup> L. Allen and G.I. Peters, *J. Phys. A: Gen. Phys.* **5**, 546 (1972).
- <sup>15</sup> J. Keaveney, A. Sargsyan, D. Sarkisyan, A. Popoyan, and Ch. Adams, *J. Phys. B*, **47** (2014) 075002
- <sup>16</sup> Y.-S. Lee and H. S. Moon, *Opt. Express*, **24**, 10723 (2016).
- <sup>17</sup> H. Ohadi, M. Himsworth, A. Xuereb, and T. Freegarde, *Opt. Express* **17**, 23003 (2009)
- <sup>18</sup> L. S. Vasilenko, V. P. Chebotaev, and A. V. Shishaev, *JETP Lett.* **12**, 113 (1970).
- <sup>19</sup> R. Hamid, M. Cetintac, and M. Celik, *Opt. Commun.* **224**, 247 (2003).
- <sup>20</sup> S. V. Kargapol'tsev, V. L. Velichansky, A. V. Yarovitsky, A. V. Taichenachev, and V. I. Yudin, *Quant. Electron.* **35**, 591 (2005).
- <sup>21</sup> M. Parniak, A. Leszczynski, and W. Wasilewski, *Appl. Phys. Lett.* **108**, 161103 (2016).
- <sup>22</sup> B. DeBoo, D. K. Kimball, C.-H. Li, and D. Budker, *JOSA B* **18**, 639 (2001).
- <sup>23</sup> R. Salomaa and S. Stenholm, *J. Phys. B: At. Mol. Opt. Phys.* **8** 1795 (1975)
- <sup>24</sup> R. Salomaa and S. Stenholm, *J. Phys. B: At. Mol. Opt. Phys.* **9** 1221 (1976)
- <sup>25</sup> A. M. Akulshin, A. A. Orel, and R. J. McLean, *J. Phys. B: At. Mol. Opt. Phys.* **45**, 015401 (2012)
- <sup>26</sup> A. M. Akulshin, B. V. Hall, V. Ivannikov, A. A. Orel, and A. I. Sidorov, *J. Phys. B: At. Mol. Opt. Phys.* **44**, 215401 (2011)
- <sup>27</sup> D. Steck <http://steck.us/alkalidata/sodiumnumbers.1.6.pdf>
- <sup>28</sup> C. P. Pearman, C. S. Adams, S. G. Cox, P. F. Griffin, D. A Smith, and I. G. Hughs, *J. Phys. B* **35**, 5141 (2002).
- <sup>29</sup> P. G. Pappas, M. M. Burns, D. D. Hinshelwood, M. S. Feld, and D. E. Murnick, *Phys. Rev. A* **21** 1955 (1980).
- <sup>30</sup> V. Horvatic, T. L. Correll, N. Omenetto, C. Vadla, J. D. Winefordner, *Spectrochim. Acta B* **61**, 1260 (2006)
- <sup>31</sup> K. D. Bonin and T. J. McIlrath, *J. Opt. Soc. Am. B* **1**, 52 (1984).
- <sup>32</sup> A. Dogariu and R. B. Miles, *Opt. Express* **24** A544 (2016).
- <sup>33</sup> A. Laurain, M. Scheller and P. Polynkin, *Phys. Rev. Lett.* **113**, 253901 (2014).